Zárójelentés

A pályázat alapvető célja egy korszerű elektrokémiai mérőegyüttes (pásztázó elektrokémiai mikroszkóp, közkeletű rövidítéssel SECM) beszerzése, üzembe helyezése, és a feladattervben felsorolt témakörök kísérleti vizsgálata volt. A beszámolót – ennek megfelelően – részekre bontottuk.

Az SECM berendezés beszerzése

Mint azt a pályázat hosszabbítási kérelmében részletesen leírtuk, eredetileg azt terveztük, hogy a beszerzésre a projekt elején kerül sor, és így már az első évben lehetőség nyílik a kísérleti munkára. A finanszírozás három évre való széthúzása miatt (amelyet a Kémiai Kutatóközpont – az előzetes várakozások ellenére – nem tudott saját forrásból áthidalni) a berendezés beszerzésére csak a projekt eredeti futamidejének végére nyílt lehetőség. (Megjegyezzük, hogy a finanszírozás harmadik részösszegét így is a Kémiai Kutatóközpontnak kellett megelőlegeznie.) a beszerzést tovább lassította a közbeszerzési eljárás nehézkessége.

A közbeszerzési pályázatra két németországi cég adott be pályázatot, de csak egyikük pályázata bizonyult érvényesnek, ezért ez a cég (a Sensolytics) kapta a megrendelést. A vállalt határidőkhöz képest féléves csúszással helyezte üzembe a mérőegyüttes első kiépítését, és ezek után is rendszeres szoftverproblémákkal küszködtünk hónapokon át.

A megvásárolt SECM berendezés unikális komponense az ún. *shear force* (SF) modul, amely lehetővé teszi, hogy a berendezéssel a vizsgálandó felület topológiáját és elektrokémiai inhomogenitásait egymástól függetlenül vizsgáljuk. A Sensolytics a SF modult – mérnökének és laboránsának többszöri kiszállása ellenére – csak az idei év elején volt képes úgy-ahogy használható állapotba hozni. Jelenleg a SF modul csak nagyon hosszadalmas beállítási procedúrák után, elégtelen megbízhatósággal és stabilitással üzemel, ezért rutinszerű mérésekre még mindig nem alkalmas. Megjegyezzük, hogy a konkurens cégek hasonló moduljai más kutatóhelyeken hasonló problémákkal küszködnek, így a kialakult késedelmekért nem egyedül a Sensolytics felelős – a technika az előzetes várakozásokhoz képest sokkal nehezebbnek bizonyult. Nagyon nagy szerepe van a használat során a kezelő manuális ügyességének és gyakorlatának (ennek érdekében két fiatal munkatársunk egy-egy hetet töltött a Sensolytics kutatói hátterét adó egyetemen, a fogások elsajátítása érdekében).

Összességében elmondható, hogy az SECM berendezés – az SF modul kivételével – rutinszerűen használhatóvá vált a pályázati *futamidő végére.*

A makro-, mezo- és mikroszkopikus léptékű mérések integrációja

Mivel a pályázatban a radikálisan eltérő léptékű mérések integrációja volt a cél, az SECM berendezés üzembeállításának késedelme csak a a mezoszkopikus jellemzést hátráltatta – a mikroszkopikus és makroszkopikus mérések ettől függetlenül zajlottak az alábbi területeken.

- *Három dimenzióban rendezett szén nanocső-erdő felhasználása elektrokémiai szuperkondenzátor készítésére.* A projektben a drezdai Fraunhoffer-intézettel és az egyetem Fizikai Kémiai tanszékével együttműködve többtucat minta széleskörű makroszkopikus elektrokémiai jellemzését végeztük el (ciklikus voltammetria, elektrokémiai impedancia, galvanosztatikus töltés és kisütés, stabilitás- és hatásfok-vizsgálatok). Néhány szuperkondenzátor-felületet az SECM készülékben is megvizsgáltunk, és azt tapasztaltuk, hogy számottevő a laterális inhomogenitás azokban a mintákban, amelyek kisebb kapacitásúnak és rövidebb élettartamúnak bizonyultak. A SF-modul alkalmazása ezen minták esetén még nem volt sikeres, így egyelőre nem tudjuk megválaszolni, hogy az inhomogenitás kémiai és/vagy topológiai jellegű-e. A mérések részeredményeinek publikálása partnereinkkel egyeztetett módon, a közeli jövőben várható.
- *Önszerveződő monorétegek vizsgálata.* A legtöbb előzetes eredmény ezen a területen született. Az Osztály pásztázó alagútmikroszkópjával már rutinszerűen tudunk kétdimenziós felületi rétegekről atomi felbontású felvételeket készíteni (néhány ilyen felvételt illusztrációként a függelékben mutatunk). Itt elsősorban azt vizsgáljuk, hogy a felületi rétegben a tömbfázishoz képes milyen új szerkezetek jelennek meg, ezeket mennyiben határozza meg az alattuk lévő szubsztrát szerkezete és milyen stabilitással rendelkeznek. Az SECM mérések ezeken a rendszereken is elkezdődtek, avval a céllal, hogy a rétegeket elektrokémia litográfiás maszkként használhassuk, és az SECM mikroelektródjával lokális felületmódosításokat végezhessünk mikroszkopikus bioszenzorok kialakítása céljából. A munka ugyancsak együttműködésben folyik, és az első publikáció kb. fél év múlva várható.
- *Lokalizált korrózió tanulmányozása.* Az előzetes várakozással szemben a berendezés zajszintje és érzékenysége csak a kifejlett lyukkorróziós aktivitás követésére bizonyult megbízhatóan alkalmasnak, a metastabil pitting detektálása éppen a berendezés teljesítőképességének határán van. Ezen a területen ezért az érzékenység növelését és a zajszint csökkentését tűztük ki célul, amely saját forrásból, az intézeten belüli szakértelem felhasználásával lehetségesnek látszik.

Az elvégzett munkáról összefoglalásképpen megállapíthatjuk, hogy a tanulmányozni kívánt rendszerek makroszkopikus jellemzése megtörtént (elsősorban elektrokémiai és spektrális ellipszometriai technikákkal), és az atomi szintű jellemzés is rutinszerűen megy a pásztázó alagút és atomi erőmikroszkópok segítségével. A mezoszkópikus tartomány vizsgálata a berendezés kései installációja és szoftverproblémái miatt csak néhány hónapja folyik normális mértékben, ezért publikációk elkészültéről még nem tudunk beszámolni.

Függelék. Sztearinsav és arachidinsav mintázata

1:1 sztearinsav és arachidinsav, 1nA 600 mV

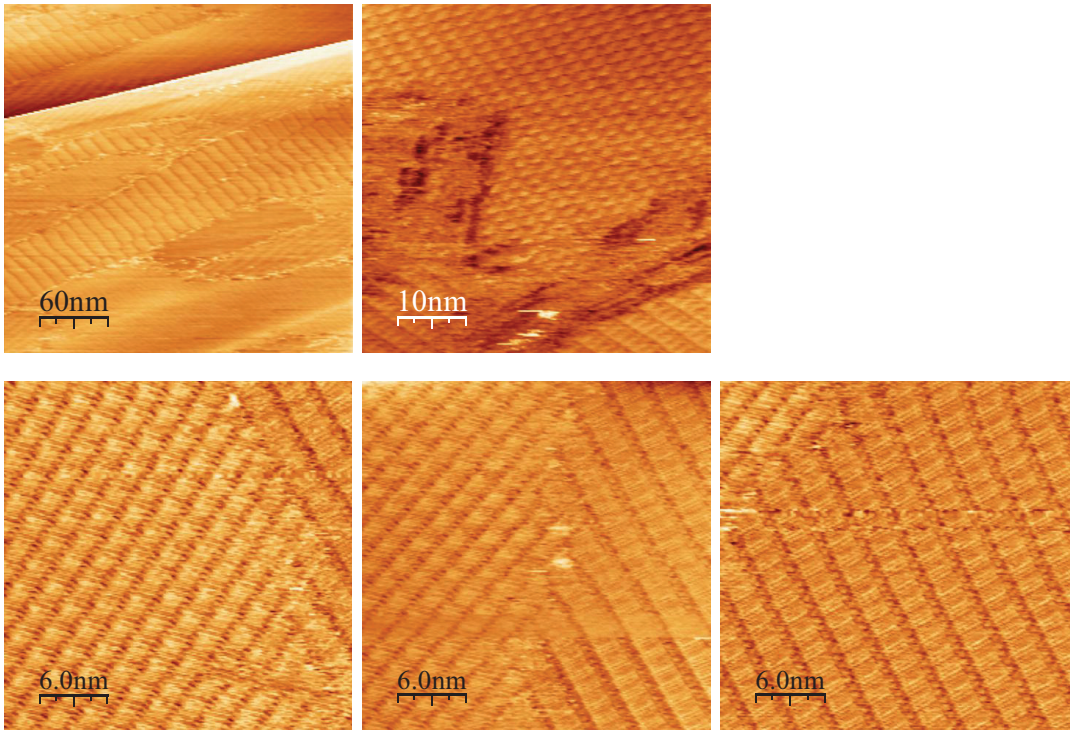

Kiegészítés a 68997 sz. OTKA pályázat zárójelentéséhez

Az alábbiakban röviden összefoglaljuk az elmúlt évben elvégzett munkát, és mellékeljük azon két munka kéziratát, amelyek már közlési stádiumba jutottak.

A technikai feltételekről annyit jegyzünk meg, hogy a berendezés – számtalan szoftverhiba korrekciója után – már megbízhatóan működik. Az egységhez tartozó bipotenciosztát a mérőegyüttes leggyengébb komponense (viszonylag magas zajszint és szerény érzékenység miatt), ezért saját forrásból extrém alacsony zajú (50 fA rms) és nagy érzékenységű, logaritmikus árammérővel ellátott bipotenciosztátot készíttetünk hozzá, amely elkészült, és jelenleg a meglévő rendszerhez való szoftveres illesztése folyik.

A beszámolási időszakban előrelépés az alábbi három területen történt.

A korrózióvédő bevonatok sérülése esetén károsodik a védendő alapfém. Ennek megelőzésére a legkorszerűbb eljárás ún. öngyógyító bevonatok alkalmazása, amelyek aktív vagy passzív módon kijavítják a bevonaton esett sérülést. A pásztázó elektrokémiai mikroszkóppal acélra fölvitt epoxi-bevonatokat tanulmányoztunk, amelyek mikrokapszulákba zárt lenolajat tartalmaztak. A bevonat sérülése esetén a mikrokapszulák felnyílnak, és tartalmuk a levegő oxigénjének hatására térhálósodik, így spontán hozva létre új bevonatot a sérült helyeken. A sérüléseket karcolással modelleztük, és összehasonlítottuk a kapszulákat nem tartalmazó bevonatok viselkedését az öngyógyító bevonatokkal. A pásztázó elektrokémiai mikroszkóppal a sérülések mikroszkopikus környezetében fennálló Fe^{2+} és oldott oxigén koncentrációját követtük az idő és a hely függvényében. Amint a mellékelt, közlésre benyújtott kéziratban kifejtjük, az öngyógyító bevonat jelentős mértékben csökkentette a bevonat sérülésének hatását, és a pásztázó elektrokémiai mikroszkóp a folyamatok követésére hatékony eszköznek bizonyult.

A másik mellékelt cikkben új korróziós inhibítorok hatását vizsgáljuk pásztázó elektrokémiai mikroszkóp, elektrokémiai kvarckristályos nanomérleg és impedancielemzés segítségével.

A harmadik területen a feladat összetettsége miatt nem tartunk még a publikálható eredmények szakaszában. Itt mikroelektronikai módszerekkel, szilíciumlapkákon elkészített aranyszenzorok lokális felületmódosítását végezzük oly módon, hogy a teljes felületet önszerveződő monoréteggel lezárjuk, majd a pásztázó elektrokémiai mikroszkóp mikroelektródjával litográfiát végzünk oly módon, hogy a kiválasztott területeket váltóáramú elektrodeszorpció révén szabaddá tesszük, ahová az oldatfázisból a kívánt felületmódosító anyag így leválasztható. A cél az, hogy az eljárás ismételt alkalmazásával különféle szenzorokat építsünk egyetlen lapkára, megvalósítva így egy *lab-on-a-chip* berendezést. A jelenlegi fázisban az első leválasztási lépés paramétereinek optimalizálásánál tartunk.

Megjegyezzük még, hogy a három dimenzióban rendezett nanocső-erdő vizsgálata, amelyet a zárójelentésben említettünk, nem hozta meg a kívánt eredményt. Mint kiderült, a felületek viselkedése alapvetően az egyfalú/többfalú naoncső-aránytól függ, az elektrokémiai mikroszkóp ennek megkülönböztetésére azonban nem alkalmas.

Az önszerveződő monorétegek korábban leírt vizsgálatai a mikroelektródos litográfia projektben hasznosulnak.

Budapest, 2011. november 28.

Nyikos Lajos

Mellékletek:
SECM study of steel corrosion under scratched microencapsulated epoxy resin
Electrochemical studies of thiazole derivatives inhibition effect against copper corrosion in acidic media

SECM study of steel corrosion under scratched microencapsulated epoxy resin

A. Pilbáth, T. Szabó, J. Telegdi, L. Nyikos

Chemical Research Center of the Hungarian Academy of Sciences,
Institute of Nanochemistry and Catalysis
HU-1025 Budapest, Pusztaszeri út 59-67, Hungary

Corresponding author: aranka.pilbath@chemres.hu
Phone: +36-1-438-1100/545, Fax: +36-1-438-1164

Abstract

Scratch tests were performed on epoxy coated steel samples with and without microcapsulated linseed oil, known to develop a polymerized protective layer after having been released from the capsules at the damaged sites. The scanning electrochemical microscope (SECM) has been applied to monitor the protection efficiency of this self-healing coating in aqueous acidic solution. In the proximity of the local damage, both the anodic metal dissolution and the cathodic oxygen reduction showed that the coating with microcapsules substantially and spontaneously decreased the rate of corrosion proving the self-repair concept of the coating.

Keywords: SECM, corrosion, self-healing, iron dissolution, microcapsules, epoxy primer

1. Introduction

Polymeric coatings are commonly used to isolate metals from the corrosive environment, but the protection efficiency can decrease substantially if the coating is damaged. Traditionally, the only remedy was to renew or otherwise manually repair the deteriorated coating. Recently, however, the concept of self-healing, self-repairing coatings emerged in the research of functional polymers. The main objective is, preferably without manual intervention, the regeneration of the functionality of damaged, cracked coating [1]. The methods of self-healing process vary: some are autonomous, some require external stimulus like temperature increase. Special polymeric chains that are separated by cracking or scratching can reconnect, building up a physical network by intrinsic (chemical/physical interactions) or extrinsic (healer-loaded tubes, fibres, capsules) repairing effects [1]. Hollow carriers, microcapsules containing polymerizable materials like epoxy resin [2], dicyclopentadiene [3, 4], air-drying oil [5] when damaged, break together with the coating, releasing the fluid material. This liquid fills up discontinuities and soon fixes the polymer by initiator, catalyst, latent hardener [3, 6] or other reagent, e.g. air-oxygen [7]. The most explored self-repairing bulk phases are epoxy [3, 4, 8-10] and polyester matrices [11]. Self-healing microcapsules and slow release microspheres in paints studied by several authors [12] showed that microcapsules built in paint loose their core material which fills the scratch line and so the corrosion damage is diminished by an autonomous self-healing mechanism [13].

There are a few quantitative methods to investigate the defensive, anti-corrosive effect of these coatings [14]. The scanning electrochemical microscope (SECM) [15] has been introduced to the corrosion field, giving valuable microscopic information from a corroding surface [16-19] allowing the measurement of local differences in electrochemical reactivity [20] or pH [21-23] of the scanned surface [24]. With the SECM, by adequately selecting the potential applied to the ultramicroelectrode tip, scanned over the damaged area, both the release of metal ions at the anodic sites and the consumption of oxygen at cathodic sites can be monitored [25, 26] at a localized damage site where these anodic and cathodic processes occur in near proximity. The important advantage of the SECM technique is that operates on both insulating (coated) and conducting (non-coated) surfaces, thus allowing one to easily distinguish between the coated and scratched surfaces [27]. The SECM, operating in redox competition mode allows us to monitor *in-situ* the corrosion taking place within a coating defect [28]. The deterioration of organic coatings through a defect on metallic surfaces [27, 29, 30, 31], the spontaneous deterioration of the organic coatings on different metals [31, 32, 33] and the defect repair in self-healing, shape-memory polymer coating [34], and encapsulated silyl esther [35], coil-coated cladding [36] were all monitored by the SECM technique.

Here we show an example for SECM characterization of steel corrosion under scratched epoxy resin coating, with or without encapsulated linseed oil incorporated in the resin. Linseed oil, a mixture of triglyceride esters of unsaturated fatty acids, upon drying in air, is known to form a strong, continuous film due to its oxidative degradation and cross-linking [37]. It is, therefore, an ideal candidate to study autonomous self-healing.

In this paper we report the results of SECM experiments which follow the spontaneous corrosion process occurring at scratched steel surfaces, without and with the protective microcapsulated healing agent. The spontaneous corrosion protection of encapsulated microcapsules embodied into the epoxy primer has been monitored. The scratched surfaces were visualized by scanning electron microscope and by optical/fluorescence microscope.

2. Experimental

2.1. Materials, sample preparation

The chemicals used for preparation of *microcapsules* were as follows:
a) Shell-forming materials: urea (Fluka, p.a.), resorcinol (Reanal, purum), formaldehyde (Sigma-Aldrich, purum, 37%); ammonium-chloride (Reanal, purum); polyvinyl alcohol (PVA) - surfactant (Reanal, purum); b) film forming material – linseed oil (Aldrich, purum).
Microcapsules for self-healing coatings were made by emulsion polymerization. In a 200 ml beaker 1.250 g urea, 0.125 g resorcinol, 0.125 g ammonium chloride was dissolved in 65 ml of 2 % aqueous solution of PVA and 15 ml linseed oil was emulsified with sonication for 5 min (at 24 kHz, with a S7 size microtip). Then the emulsion was stirred at 600 rpm and 3.210 g of formaldehyde was added to the emulsion. The temperature of the reaction mixture was raised to 70°C at rate of 1°C/min and this temperature was kept together with stirring for 5 hrs. After cooling down to room temperature the capsules were separated, washed with diluted ethanol or with aqueous surfactant solution to remove encapsulated oil. The capsules were then dried in room temperature.
The used two-component *epoxy* wax was purchased from Ablonczy Ltd. Hungary. Resin 'A' and hardener 'B' components were mixed at a volume ratio of 25 to 1.
Experiments were performed on steel sheets. The composition of the *steel sheets* was determined by EDX measurements and the results given in at% are as follows: Fe (88.6 ± 0.7), C (10.8 ± 0.6) and Al (0.6 ± 0.1).
Wet grinding on silicon carbide abrasive papers (220-4000 grit) was used as surface preparation prior to coating. The steel sheets were ultrasonically cleaned and rinsed with acetone. Finally the samples were dried in argon flow.

Sample preparation steps were as follows:
1. The microcapsules were mixed into the resin in 4 w/w %.
2. The steel plates were covered (painted) with a brush with the above mentioned mixture and with the epoxy without microcapsules. The thickness of the dry coating was about 50-60 µm.
3. Scratches of either 20 or 200 µm width were produced in the coating on the metal substrate by a scalpel or by a sharp needle.

The coated and scratched samples were immersed in aerated aqueous solution of 1 M $NaClO_4$ and and 1 mM $HClO_4$ at room temperature, and examined *in-situ* with the SECM across the scratch. The pH of the electrolyte solution was 2.83.

The specimen was left unbiased at its open-circuit corrosion potential for all experiments. Experiments were conducted at ambient temperature.

2.2. Experimental methods

The structure, diameter and the morphology of the microspheres and the scratched surface were visualized by scanning electron microscope (SEM, Zeiss EVO 40 XVP) as well as by optical/fluorescence microscope (Zeiss Axio Imager A1); sonicator applied in emulsification was a Hielscher ultrasound technology UP200S.
The Scanning Electrochemical Microscope used was a model of Sensolytics Base SECM (Bochum-Germany). The SECM instrument was operated with a 10 µm platinum tip as the probe, a Ag/AgCl/KCl (saturated) reference electrode and a platinum counter electrode. All potential values are referred to the Ag/AgCl/KCl (saturated) reference electrode.

3. Results and discussion

Fig. 1 presents the structure, size and the morphology of the microspheres visualized by scanning electron microscope.

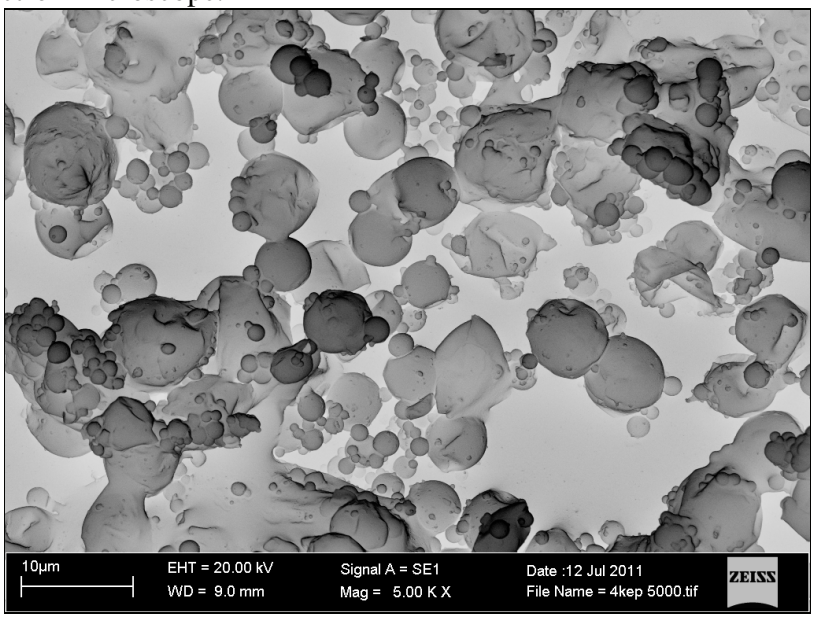

Fig. 1. SEM micrograph of urea-formaldehyde microcapsules

The diameter of the microcapsules was between 3 and 10 microns with a narrow size-distribution peaked at about 6 microns. The fluorescence microscopy pictures of the scratched samples (cf. Fig.2) show the wide and narrow scratch morphology. The green dots in the resin matrix are the microcapsules.

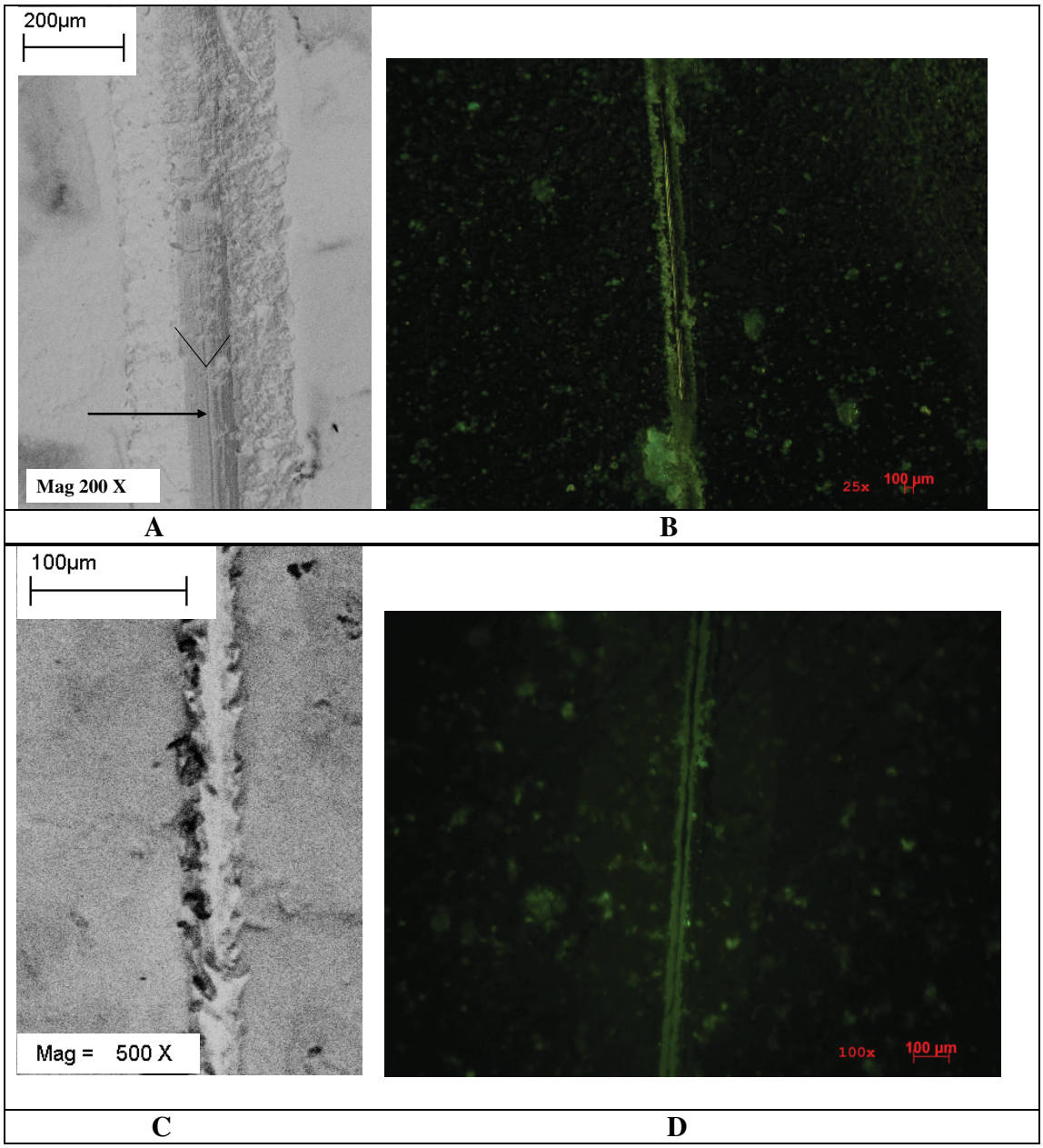

Fig. 2. SEM images (A,C) and fluorescence micrographs (B,D) taken of a scratched surface of the microcapsule-containing epoxy resin on the coated steel samples (scratch width: ~ 200 µm (A, B) and ~20 µm (C, D)

Prior to each SECM scanning experiment, the tip-sample distance was established by approach curves performed above the insulating part of the coating at -0.70 V, showing negative-feedback behavior.

The status of a scratched sample was studied by monitoring the oxidation of dissolved Fe^{2+} and reduction of oxygen (cf. Fig. 3-4) in test solutions. Corrosion activity is observed from 10 minutes immersion time in the electrolyte solution.

The process of oxidation of Fe^{2+} is not the best choice after long time explosure into the electrolyte solution because the current decrease reasonably rapidly. This can be due to the precipitation of corrosion products, which block the active zones and hinder the electrochemical activity of Fe^{2+} ions. Nevertheless, the dissolution of Fe^{2+} ions can be followed for at least two hours for both the wide and the narrow scratch (Figs. 3 and 4).

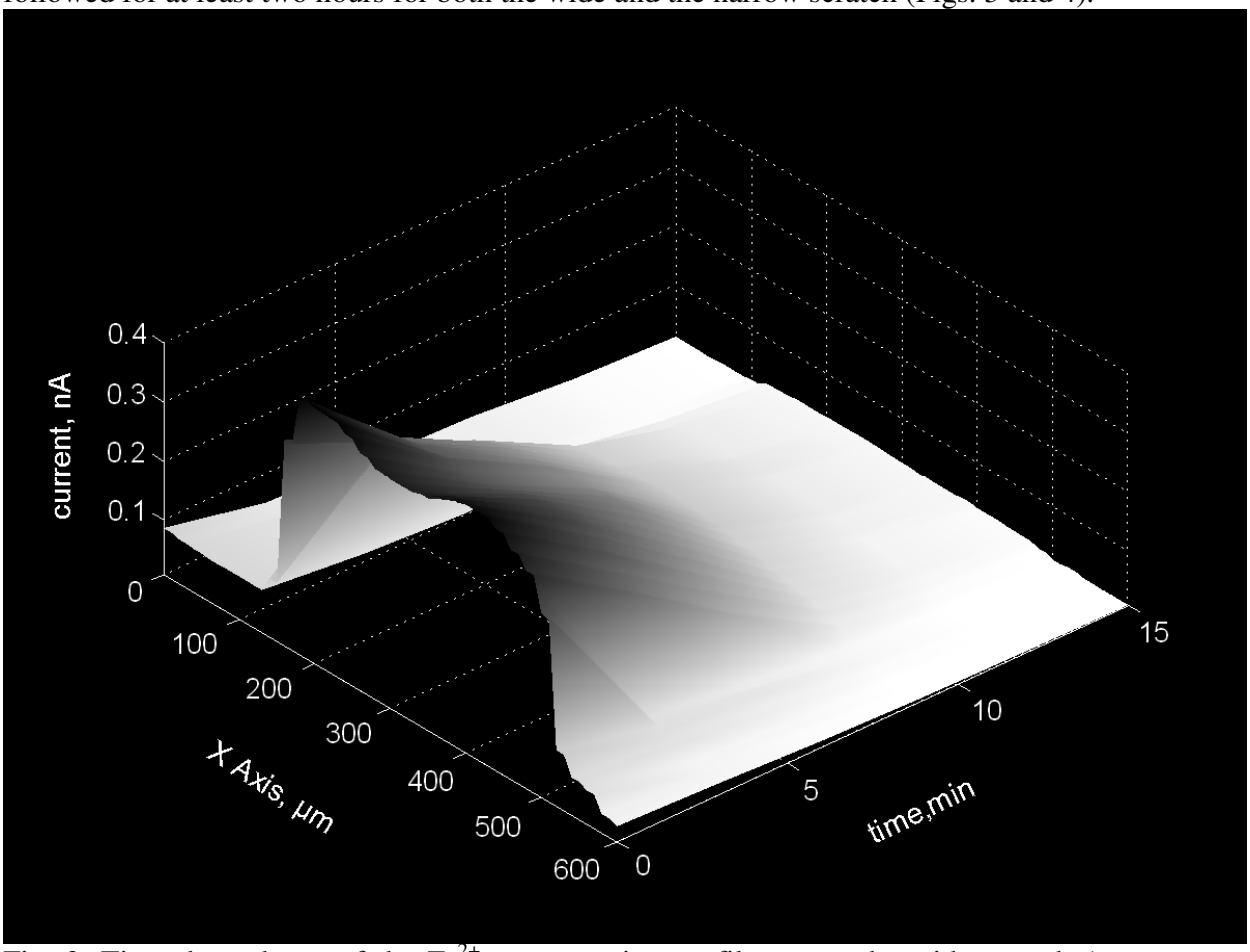

Fig. 3. Time dependence of the Fe^{2+} concentration profile across the wide scratch (no microcapsules). Tip potential 0.5 V *vs* Ag/AgCl/KCl(saturated) reference electrode

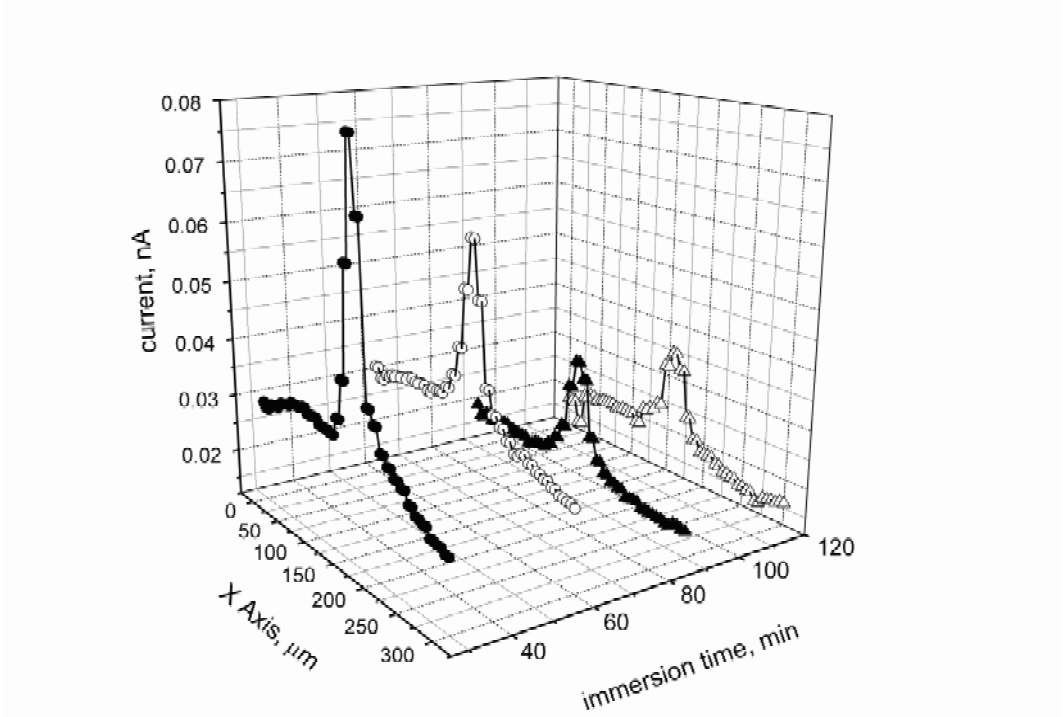

Fig. 4. 3D plot of line scans performed by SECM at different immersion time in the electrolyte solution on an epoxy coated and narrow scratched (20 µm) steel sample. The Fe^{2+} oxidation process is monitored. Immersion time: 30 min (●), 60 min (○), 90 min (▲), 120 min (Δ)

The other possibility to follow the corrosion process is to set the tip potential to that of oxygen reduction. By doing so, one initiates a competition for oxygen: oxygen is both consumed by the corrosion process and by the microelectrode. As shown in Fig. 7, oxygen concentration reaching the tip is very low above the scratch indicating a vigorous corrosion process. It can also be seen that as time passes, oxygen concentration decreases further and further away from the damaged site as oxygen is depleted more and more.

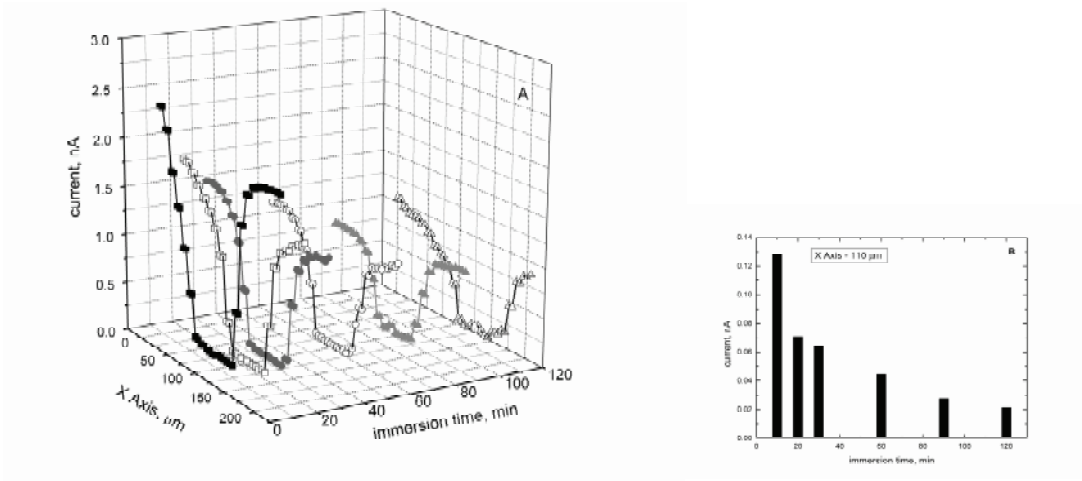

Fig. 5. A: 3D plot of line scans performed by SECM at different immersion time in the electrolyte solution on an epoxy coated and scratched (20 µm) steel sample. The oxygen reduction process is monitored. Immersion times: 10 min (■), 20 min (□), 30 min (●), 60 min (○), 90 min (▲), 120 min (Δ) B. The time dependence of oxygen reduction current measured in the middle of the scratch

The current of oxygen reduction (cf. Fig.5) measured in the middle of the scratch shows a decreasing tendency, not apparent at the scale of Fig.5A, indicating accelerating corrosion even after 2 hours.
Comparing the currents across the scratch on a sample when the microcapsules were incorporated in the coating with the reference sample (no microcapsules) shows the protection effect the linseed oil, released from the broken capsules, is able to produce.

By monitoring Fe^{2+} oxidation, the protective effect of the self-healing coating is obvious (Fig. 6). Since, as discussed above, this oxidation current is not a reliable measure of the rate of corrosion at longer times due to insoluble precipitation formation, the oxygen reduction currents are to be monitored.

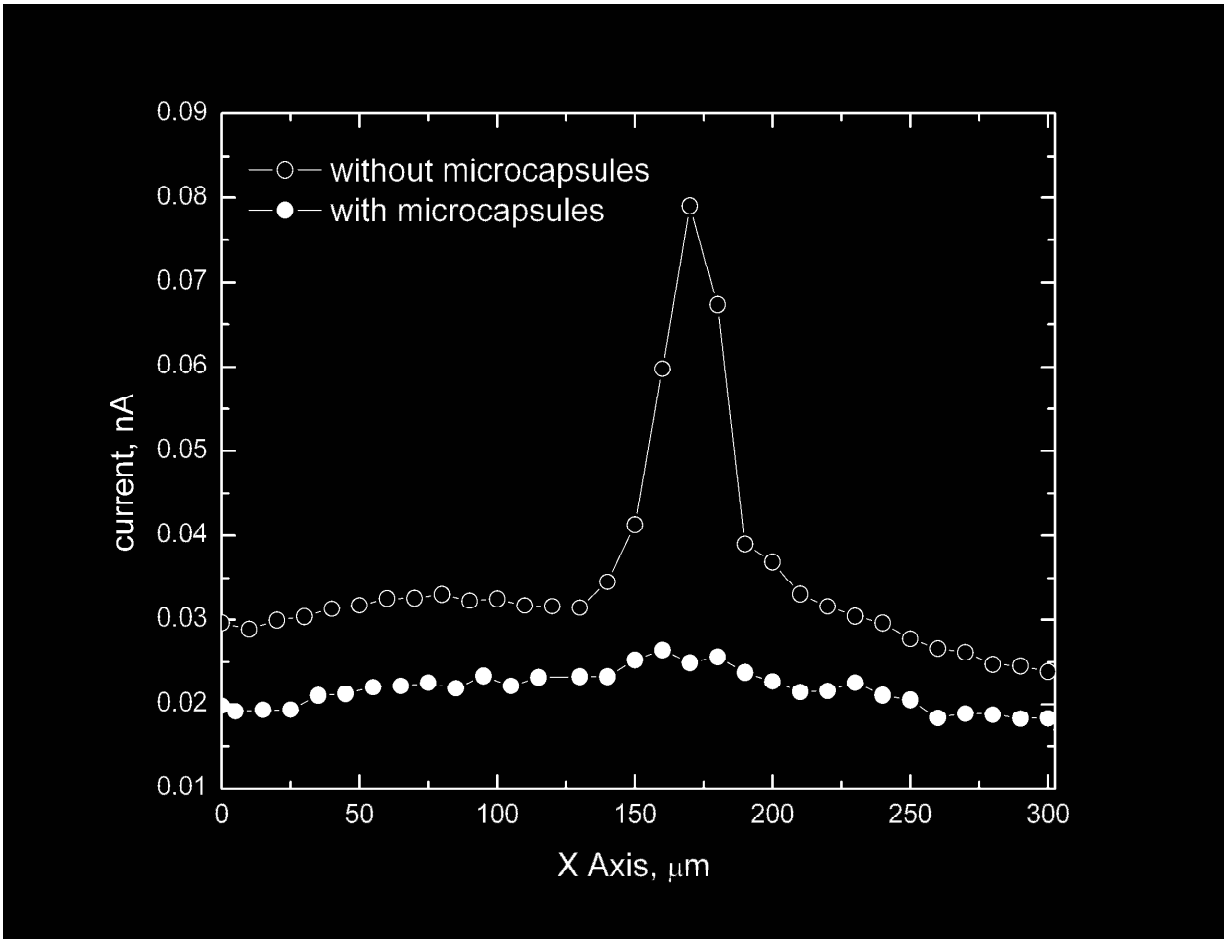

Fig. 6. Line scans performed at 30 min immersion time in the electrolyte solution on a scratched (scratch width: 20 μm) epoxy coated (opened symbols) and a scratched microcapsules embodied epoxy coated steel sample (filled symbols).

The corrosion rate, as indicated by the local oxygen consumption, is considerably lower in the microcapsule-protected sample (Fig. 7). By measuring maps, of which an example is shown in Fig. 8, it was proven that the protection effect is fairly uniform along the scratch, *i.e.* there are no unprotected areas left, thereby validating the capsule density and linseed oil quantities used in the coatings.

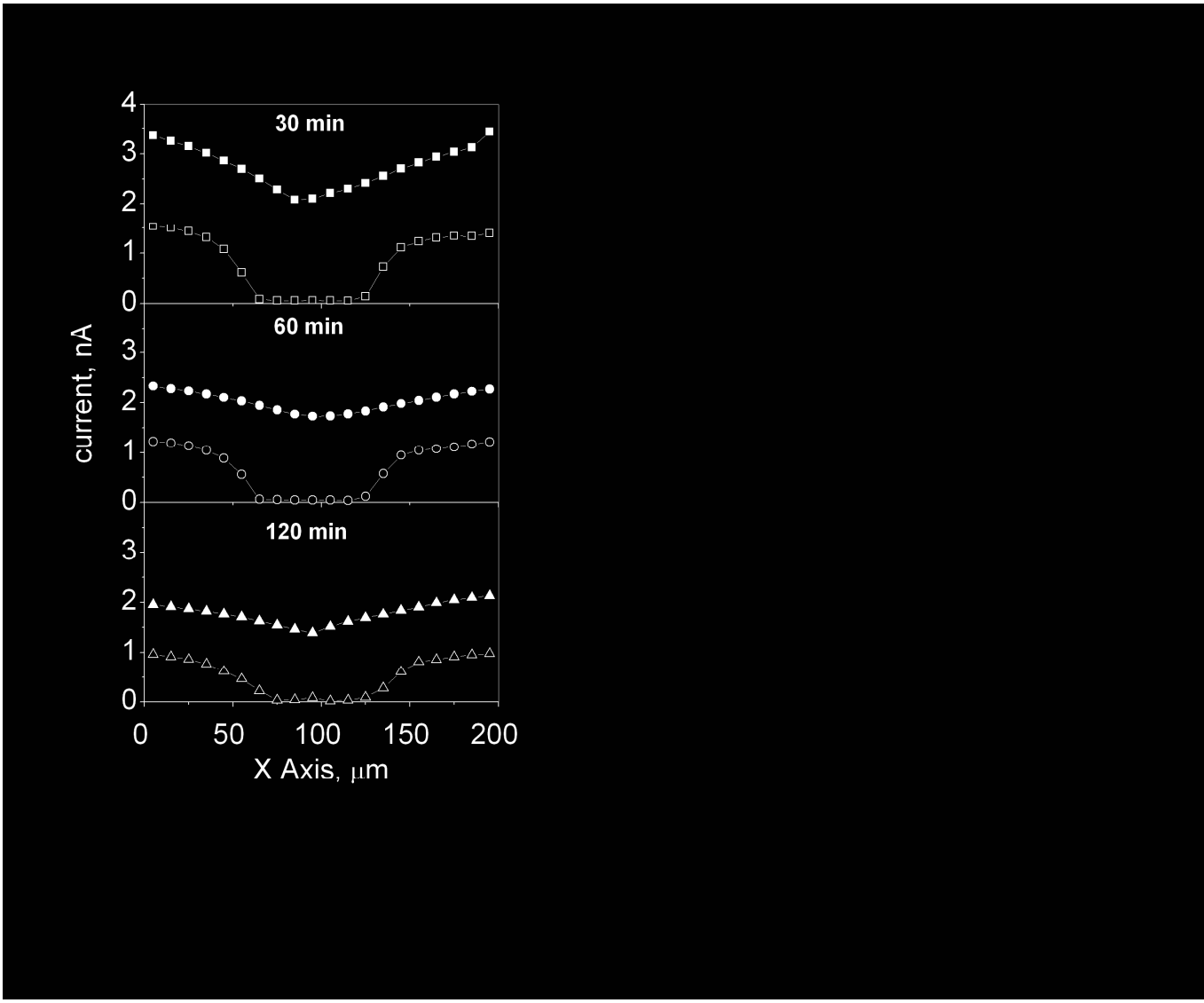

Fig. 7. Plots of line scans performed by SECM at different immersion times (indicated on the figure) in the electrolyte solution on a scratched (scratch width: 20 μm) epoxy coated (filled symbols) and a microcapsules embodied epoxy coated steel sample (open symbols). The oxygen reduction process is monitored.

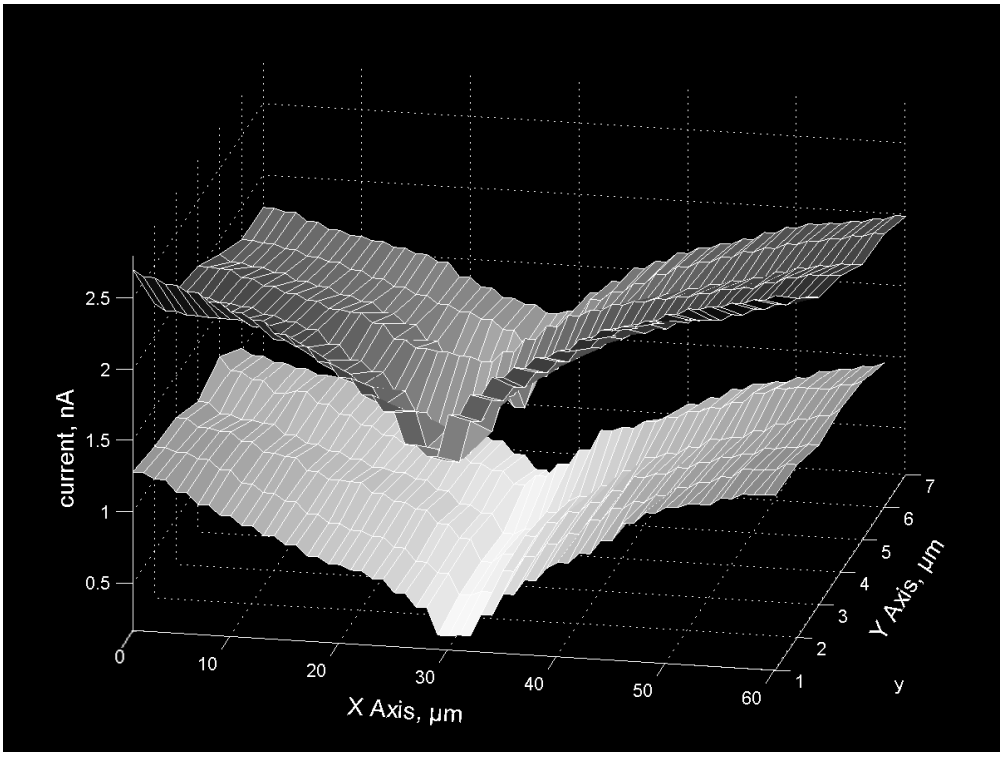

Fig. 8. Topographic map of the corrosion process in time after 2 hour immersion in the electrolyte on a coated steel sample (A - no microcapsules, B - microcapsules) with a 20 µm wide scratch.

Conclusion

The present study demonstrates that the SECM is a suitable technique to visualize and to investigate the processes of self-healing in coated steel samples. The protective effect of the microcapsule incorporated linseed oil along the scratched surface of the steel was followed. The SECM tip measured the oxidation and reduction current participating in the corrosion process. By comparing the corrosion-produced Fe^{2+} concentration and the oxygen consumption in scratched samples with and without microcapsulated linseed oil, it was established that the capsulated material shows self-healing indeed. Our next plan is to incorporate corrosion inhibitors in the microcapsules, which together with the linseed oil can cause an even more pronounced protection against corrosion caused by coating damage.

Acknowledgements

This work was supported by the Grant OTKA under project number of NK 68997.
The authors would like to express their thanks to Dr. P. Németh, Dr. L. Szabó and E. Drotár for the SEM-EDX measurements.

References

1. M.Q. Zang, Polymer Letters 2 (2008) 238
2. L. Yuan, G. Liang, J.Q. Xie, L. Li, J. Guo, Polymer 47 (2006) 5338
3. M.R. Kessler, N.R. Sottos, S.R. White, Composites: Part A 34 (2003) 743
4. S.R. White, N.R. Sottos, P.H. Geubelle, J.S. Moore, M.R. Kessler, S.R. Sriram, E.N. Brown, S. Viswanathan, Nature 409 (2001) 794
5. A. Kumar, L.D. Stephenson, J.N. Murray, Prog. Org. Coat. 55 (2006) 244
6. T. Yin, M.Z. Rong, M.Q. Zhang, G.Ch. Yang, Composites Science and Technology 67 (2007) 201
7. C. Suryanarayana, K.Ch.Rao, D. Kumar, Prog. Org. Coat. 63 (2008) 72
8. E.N. Brown, M.R. Kessler, N.R. Sottos, S.R. White, Journal of Microencapsulation 20(6) (2003) 719
9. C.L. Mangun, A.C. Mader, N.R. Sottos, S.R. White, Polymer 51 (2010) 4063
10. T. Nesterova, K. Dam-Johansen, S. Kiil, Prog. Org. Coat. 70 (2011) 342
11. D. Jung, A. Hegeman, N.R. Sottos, P.H. Geubelle, S.R. White, Compos. Funct. Grad. Mater. 80 (1997) 265
12. M. Samadzadeh, S. Hatami Boura, M. Peikari, S.M. Kasiriha, A. Ashrafi, Prog. Org. Coat. 68 (2010) 159
13. T. Szabó, L. Molnár-Nagy, J. Bognár, L. Nyikos, J. Telegdi, Prog. Org. Coat. 72 (2011) 52
14. K. Mehta, M.N. Bogere, Prog. Org. Coat. 64 (2009) 419
15. A.J. Bard, M.V. Mirkin (Eds.), Scanning Electrochemical Microscopy, Marcel Dekker, New York, 2001
16. Y. González-Garcia, G.T. Burstein, S. Gonzalez, R. M. Souto, Electrochemistry Communications, 6 (2004) 637
17. R.M. Souto, Y. Gonzalez-Garcia, S. Gonzalez, G.T. Burstein, Corr. Sci. 46 (2004) 2621
18. R.M. Souto, Y. Gonzalez-Garcia, S. Gonzalez, Corr. Sci. 47 (2005) 3312
19. R.M. Souto, Y. Gonzalez-Garcia, A.C. Bastos, A.M. Simões Corr. Sci. 49 (2007) 4568
20. A.M. Simões, A.C. Bastos, M.G. Ferreira, Y. Gonzalez-Garcia, S. Gonzalez, R.M. Souto, Corr. Sci. 49 (2007) 726
21. J. Izquierdo, L. Nagy, A´ Varga, J.J. Santana, G. Nagy, R.M. Souto, Electrochim. Acta (2010) doi:10.1016/j.electacta.2011.07.076
22. S.V. Lamaka, M. Taryba, M. F. Montemor, H.S. Isaacs, M.G.S. Ferreira, Electrochem. Commun. 13 (2011) 20
23. O.V. Karavai, A.C. Bastos, M.L. Zheludkevich, M.G. Taryba, S.V. Lamaka, M.G.S. Ferreira, Electrochim. Acta 55 (2010) 5401
24. A. Méndez-Vilas, J. Díaz, Microscopy: Science, Technology, Applications and Education, Microscopy Book Series No. 4, Formatex Research Center Publisher, Vol.3, 2010
25. A.C. Bastos, A.M. Simões, S. González, Y. González-García, R.M. Souto, Electrochem. Commun. 6 (2004) 1212
26. J.J. Santana, J. Gonzáles-Guzmán, L. Fernández-Mérida, S. Gonzáles, R.M.Souto, Electrochim. Acta 55 (2010) 4488
27. A.C. Bastos, A.M. Simões, S. Gonzáles, Y. Gonzáles-García, R.M. Souto, Prog. Org.

Coat. 53 (2005) 177
28. M. Arca, A.J Bard, B.R. Horrocks, Th.C. Richards, D.A. Treichel, Analyst 119 (1994) 719
29. J.J. Santana, J. Gonzáles-Guzmán, J. Izquierdo, S. Gonzáles, R.M. Souto, Corr.Sci. 52 (2010) 3924
30. R.M.Souto, Y. González-García, S. González, Corr.Sci. 50 (2008) 1637
31. R.M. Souto, Y. Gonzáles-García, S. Gonzáles, Prog. Org. Coat. 65 (2009) 435
32. R.M. Souto, Y. González-García, J. Izquierdo, S. González, Corr.Sci. 52 (2010) 748
33. R.M. Souto, J.J. Santana, L. Fernández-Mérida, S. González, Electrochim. Acta (2011) doi:10.1016/j.electacta.2011.03.077
34. Y. Gonzáles-García, J.M.C. Mol, T. Muselle, I. De Graeve, G. Van Assche, G. Scheltjens, B. Van Mele, H. Terryn, Electrochemistry Communications 13 (2011) 169-173
35. Y. González-García, S.J. García, A.E. Hughes, J.M.C. Mol, Electrochem. Commun. (2011) doi: 10.1016/j.elecom.2011.07.009
36. R. M. Souto, B. Normand, H. Takenouti, M. Keddam, Electrochim. Acta 55 (2010) 4551
37. M. Lazzari, O. Chiantore, Polymer Degradation and Stability 65 (1999) 303

Electrochemical studies of thiazole derivatives inhibition effect against copper corrosion in acidic media

Gy. Vastag*, A. Shaban, I. Kék, A. Pilbáth , L. Nyikos

Department of Surface Modifications and Nanostructures
Chemical Research Center, Hungarian Academy of Sciences
1025 Budapest, Pusztaszeri út 59-67, Hungary
*University of Novi Sad, Faculty of Natural Sciences and Mathematics, Yu.

SUMMARY

Corrosion and inhibition processes can be followed by different In-situ methods at a nanometer scale. In this work, the electrochemical behavior of copper in acidic sulphate containing media, without and with the addition of thiazole derivatives, was evaluated using electrochemical and electro-gravimetrical methods such as: EIS, SECM and EQCM.

The effectiveness of thiazole derivatives, in an aggressive solution of 0.1 M Na_2SO_4, on the value of the breakdown potential of the copper electrode, was investigated. The investigated thiazole derivatives are: 5-benzylidene-2,4-dioxo tetrahydro-1,3-thiazole (5-BDT) 5-(4'-isopropylbenzylidene)-2,4-dioxotetrahydro-1,3-thiazole (5-IPBDT), 5-(3'-thenylidene)-2,4-dioxotetrahydro-1,3-thiazole (5-TDT) and 5-(3',4'-dimetoxybenzylidene)-2,4-dioxotetrahydro-1,3-thiazole (5-MBDT). The inhibitor effectiveness was monitored and corrosion rates were determined.

The inhibitive effects of the tested thiazole derivatives were confirmed. The most effective, among the tested thiazole derivatives against copper corrosion, was 5-IPBDT, due to the presence of the isopropyl functional group**.**

KEY WORDS: Corrosion inhibitors; Copper; SECM, Electrochemical quartz crystal nanobalance; Corrosion breakdown potential.

Background:

Copper is a relatively noble metal, however, it is susceptible to corrosion by acids and strong alkaline solutions, especially in the presence of oxygen or oxidants [1]. In the pH range between 2 and 5 the dissolution of Cu is very rapid and the formation of a stable surface oxide layer, which can passivate metal surfaces, is impossible. Copper can only passivate by forming an oxide surface layer in weak acid or alkaline solutions. The behavior of Cu in acidic media is extensively investigated and several schemes have been presented for the dissolution process [1-5].

The application of corrosion inhibitors in such conditions becomes a necessity, since no protective passive layer can be formed [1]. The possibility of the copper corrosion prevention, by the application of corrosion inhibitors, have been investigated by several researchers. Amongst them there are inorganic inhibitors, but in much greater numbers there are organic compounds and their derivatives such as azoles, amines, amino acids. It is worth mentioning that the presence of hetero-atoms such as nitrogen, sulphur, phosphorous in the organic compound molecule improves its action as copper corrosion inhibitor.

The role of adsorption type inhibitors can be explained by the Lewis acid-base interaction on metal surfaces. The structure of the molecule is one of the major factors that influence this interaction [2]. The molecular structure of azoles contains atoms like N and S, which are easily able to bridge with other molecules [1, 2, 6-16].

Thiazoles are members of the azoles heterocycles that includes imidazoles and oxazoles. Thiazole can also be considered a functional group. Thiazoles are structurally similar to imidazoles, with the thiazole sulfur replaced by nitrogen. The Thiazole rings are planar and aromatic and are characterized by a larger pi-electron delocalization and have therefore great aromaticity.

The thiazole derivatives molecules adsorb probably through the nitrogen or through coordination with surface from the thiazole ring and form the protecting layer. For a metal such as copper, which can form multi-bonds, inhibitor molecules containing those atoms are strongly recommended.

New methods of probing the microscopic processes on electrode surfaces have recently been developed in the field of Electrochemistry. Among them, scanning microelectrochemical techniques, which are an extension of local probe techniques originating from the use of microelectrodes as the probes in near field microscopic techniques to operate inside an electrochemical cell, are concentrating major interest. In this way, the chemical and/or electrochemical selectivities provided by the microelectrode probes can be successfully combined with the spatial resolution of the scanning microscopies, thus allowing surface characterization with a resolution in the micrometer range or even below.
Among these techniques, scanning electrochemical microscopy (SECM) was designed in 1989 by Bard and coworkers, and since then, the SECM has become a very powerful technique for probing a great variety of electrochemical processes in fundamental and applied electrochemistry, energy storage, materials science, corrosion science, biosensors research and biophysics.
In this contribution, the operation modes of SECM will be described and selected applications in the investigation of corrosion reactions will be provided in order to illustrate its application in sensing localized corrosion.
The SECM instrument basically consists of a combination of electrochemical components, positioners and computer control. The SECM is a technique in which a current flows through a microelectrode immersed in an electrolytic solution and situated close to a substrate. The substrate can either be a conductive, semiconductive or insulating material. The

microelectrode and the substrate form part of an electrochemical cell which is also constituted by reference and auxiliary electrodes, and sometimes by a second working electrode. The electrochemical setup is constituted by this electrochemical cell together with the bipotentiostat, which is the actual electrochemical interface. It allows the potential of the microelectrode and/or the substrate versus the reference electrode to be controlled, as well as to measure the current flowing between any of the working electrodes and the counter electrode. The microelectrode displacement and its position relative to the substrate are controlled with a three-dimensional microstage that provides independent and accurate control in the X-Y-Z axis. And the remaining component is the data acquisition and display system, usually conformed by a computer, an interface and a display system.

Several investigations utilized EQCM to investigate copper electrode behavior in acidic environment [12-17]. EQCM is capable of detect mass changes in the nanogram range.
Our previous results showed very promising inhibition effects for the tested thiazole derivatives.

The aim of this work is to apply the electrochemical methods such as: EIS, SECM, EQCM, in order to investigate the effectiveness of different thiazole derivatives, on copper corrosion in acidic solution.

Experimental

Electrodes:

A polycrystalline Cu (99.99%) electrode was used for the electrochemical measurements. Galvano-statically deposited copper layers were used for the EQCM studies.

Chemicals and solutions

Reagent grade chemicals (Reanal Finom vegyszergyár) and double distilled water were used to prepare the following electrolytes:

0.1 M Na_2SO_4 at pH ≅2.95
The pH was adjusted to 2.95 using diluted sulfuric acid.

Investigated inhibitors:

Thiazole derivatives:
5-benzylidene-2,4-dioxo tetrahydro-1,3-thiazole (5-BDT)
5-(4'-isopropylbenzylidene)-2,4-dioxotetrahydro-1,3-thiazole (5-IPBDT)
5-(3'-thenylidene)-2,4-dioxotetrahydro-1,3-thiazole (5-TDT)
5-(3',4'-dimetoxybenzylidene)-2,4-dioxotetrahydro-1,3-thiazole (5-MBDT)

All experiments were done at open atmosphere and room temperature. Due to the low solubility of the tested thiazole derivatives, inhibitors were first dissolved into 20 ml of ethanol and then diluted to the desired concentration. All inhibitors were tested at a concentration of 0.01 $mmol.dm^{-3}$. This concentration was found to be the optimal concentration for copper corrosion inhibition.

***SECM measurements*:**

The Scanning Electrochemical Microscope used was a model of Sensolytics Base SECM (Bochum-Germany). The SECM instrument was operated with a commercial 25 µm gold tip as the probe, a Ag/AgCl/KCl (saturated) reference electrode and a platinum counter electrode. All potential values are referred to the Ag/AgCl/KCl (saturated) reference electrode.

The substrate material was copper. Wet grinding on silicon carbide abrasive papers (220-4000 grit) was used as surface preparation prior to each measurement. The copper samples were ultrasonically cleaned and rinsed with ethanol. Finally the samples were dried in argon flow. The sample was left at its open circuit potential during the measurements. Ferrocene-methanol (hydroxymethylferrocene - FeMeOH) was used as redox-mediator.

The following materials were used as received: 5-IPBDT, sodium sulphate (Na_2SO_4 - Aldrich), hydroxymethylferrocene (FeMeOH – ABCRGmbH&Co KG).

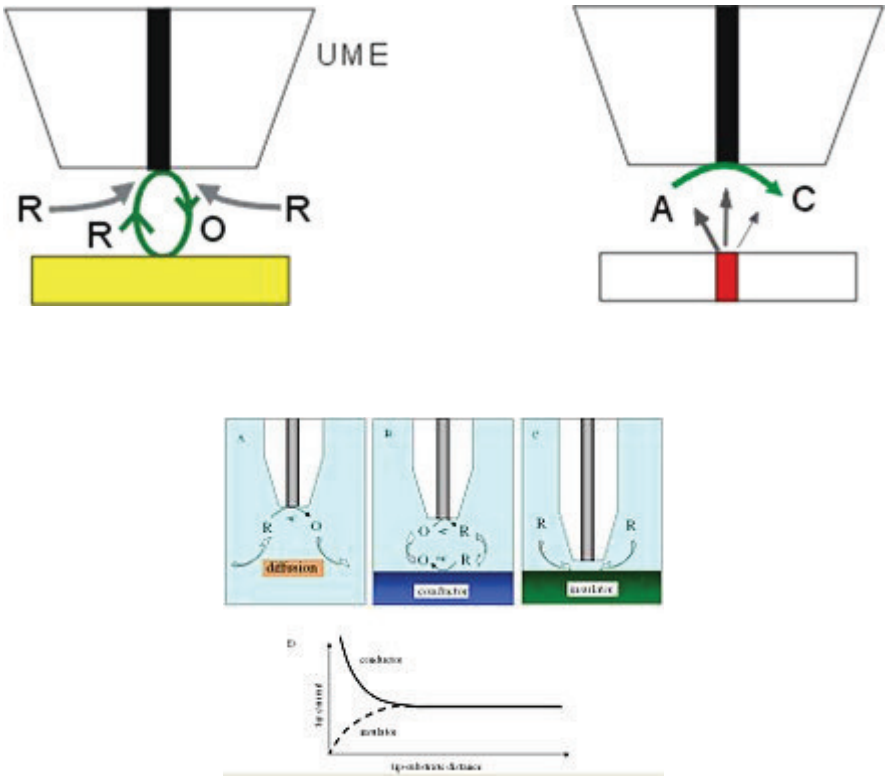

***EQCM Measurements*:**

An electrochemical quartz crystal nanobalance Model EQCN-700 (Elchema, Potsdam, NY) with 10 MHz AT-cut quartz resonators was used in this study. The EQCN technique allowed us for simultaneous monitoring of voltamperometric and resonance frequency versus potential characteristics. For thin rigid films, the interfacial mass changes are related to the changes in oscillation frequency of the EQCN through the Sauerbrey equation:

The quartz crystal applied for our investigations had gold layers deposited at both sides (thickness 150-nm) over a thin layer of Cr (thickness 15-nm, for adhesion purpose). Copper layers were galvanostatically electrodeposited on one face of the crystal, facing the solution, at room

temperature. The deposition bath contained 0.5M $CuSO_4$, 0.5M H_2SO_4, and 1M C_2H_5OH in doubly distilled water. The cell reference and counter electrodes were SCE and a Pt wire, respectively.

The active geometrical surface area of the working Au electrode, (radius = 2.55 mm), was 0.2 cm^2. It was deposited on a 13.7 mm diameter, 10 MHz AT-cut quartz resonator wafer. The resonator crystals were sealed to the side of a glass vessel. The working electrode was polarized using a Pt sheet, area = 6.5 cm^2, counter electrode and its potential measured versus saturated (KCl) calomel electrode (SCE).

The results were obtained in a simultaneous recording of *i–E* and Δ*f–E*, or *m–E* curves. During all three intervals, frequency, mass changes and surface potential changes were monitored. Data collected were analyzed and stored using specially developed software. In other electrochemical measurements, polarization measurements were performed on the freshly deposited Cu surfaces. Potential was scanned from –350 to +150 mV in both a forward and backward scans.

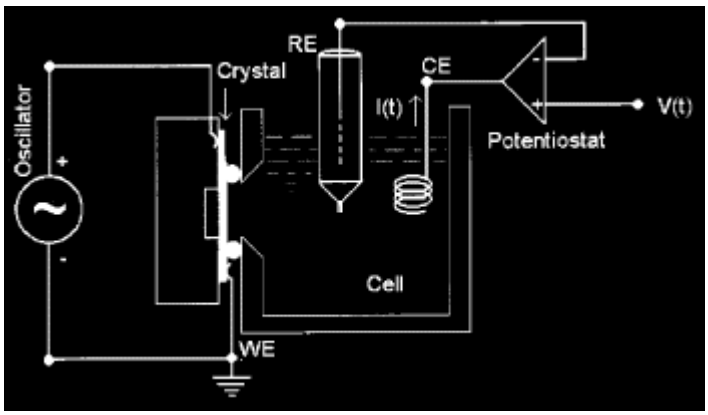

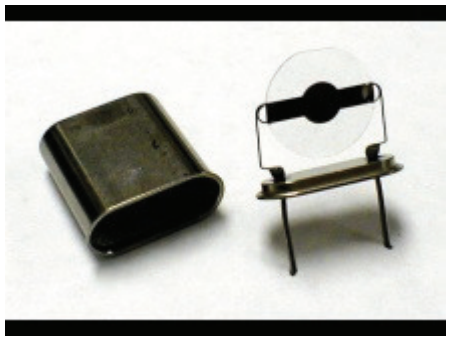

RESULTS AND DISCUSSION

EIS results

Figure 1 shows a typical electrochemical impedance spectroscopy plots (Nyquist and Bode plots) of copper electrode in 0.1M Na_2SO_4 electrolyte without and with the addition of tested inhibitors. Figure 1a shows the depicted polarization resistance values in comparison to the blank aggressive solution. The R_p values were obtained by calculating the semicircle intersection with the real part of the amplitude. It is clear that IPBDT produced the highest R_p value, which is an indication of the formation of a protective film that hindered corrosion.
The inhibition efficiency ($\eta\%$) was determined using the following formula:

$$\eta\ (\%) = (1 - R_p^{inh} / R_p^{o}).\ 100 \qquad (1)$$

where R_p^{o} and R_p^{inh} represent the electrode polarization resistance in the absence and presence of the inhibitor in the electrolyte, respectively.

Polarization resistances and inhibition efficiency results are given in Table 1. The inhibitor 5-IPBDT produced the lowest corrosion current density thus the highest inhibition efficiency against Cu corrosion (η = 93%). This can be explaining by the presence of N and S in the molecule structure and the longer chain serves as a protecting shield on the copper electrode surface.

Table 1. Polarization Resistance (R_p) and Inhibition efficiency (η) values for the tested Thiazole derivatives

Inhibitor	**IPBDT**	**BDT**	**TDT**	**MBDT**
R_p (k ohm)	**115**	**15**	**9.3**	**7.3**
Inhibitor Efficiency %	**93**	**86**	**80**	**71**

Figure 1b shows the Bode plot for the tested thiazole derivatives. Phase shift versus the log of the frequency gives an indication of the behavior of the protective film formed on the electrode surface due to the inhibitor adsorption. It can be seen from this figure that the process taking place at the electrode surface has one relaxation time constant. The location of the relaxation time constant did not change much from one inhibitor but the phase shift value increased with IPBDT having the highest value at the peak location. This is an indication that the adsorption of all inhibitors on the electrode surface follows the same pattern but with different intensities [21].
In a further study a model must be constructed to simulate the processes taking place.

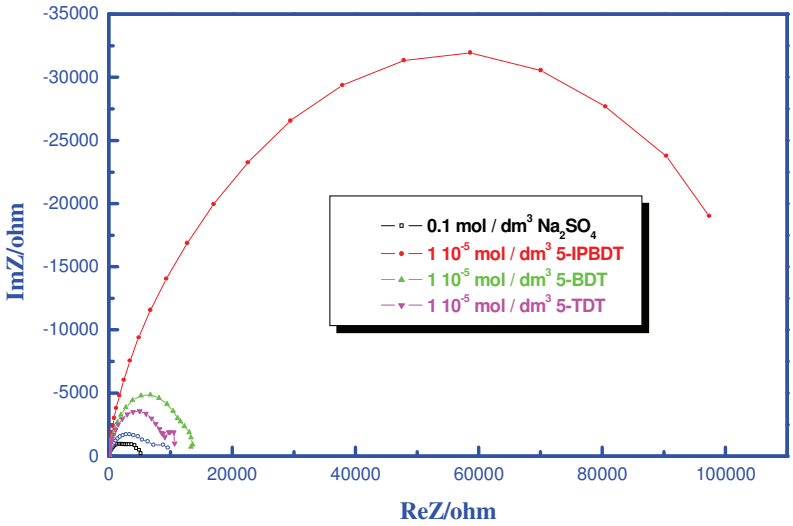

Figure 1a. Nyquist plot of EIS for the tested Thiazole derivatives

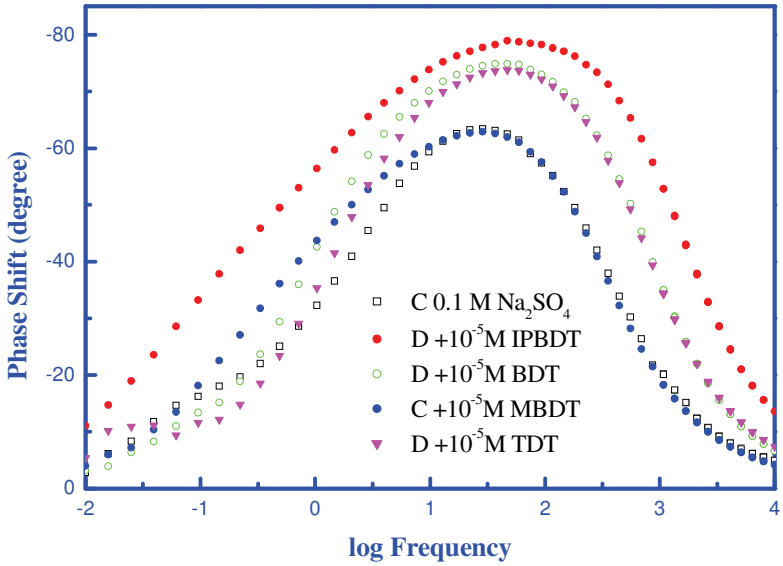

Figure 1b. Bode plot of EIS for the tested Thiazole derivatives

SECM results:

Cu in 0.1 M Na_2SO_4 solution + 5-IPBDT:

Scanning Electrochemical Microscopy (SECM) was applied to study the IPBDT inhibitor layer formation on copper surface. Approach curves of the SECM tip towards the copper surface were measured *in-situ* in IPBDT and redox-mediator containing Na_2SO_4 electrolyte with a commercial 25 µm Au electrode. The study was carried out for 3 hour, following the layer formation process.

The measurement of the approach curves were done *in-situ* at open circuit potential in a solution of 0.67 mM FeMeOH and 0.1 M Na_2SO_4 + 0.01 mM IPBDT + 0.67 mM FeMeOH.

The base approach curves were performed first in mediator solution (inhibitor and also sodium sulphate free solutions) in order to find the distance where we are close enough to the surface. The next approach curves were done in the inhibitor, sodium sulphate and electrochemical-mediator containing aqueous solutions without changing the tip position in horizontal plane. The formation of inhibitor layer was monitored *in-situ* by approach curves performed at different times, see Figure 2.

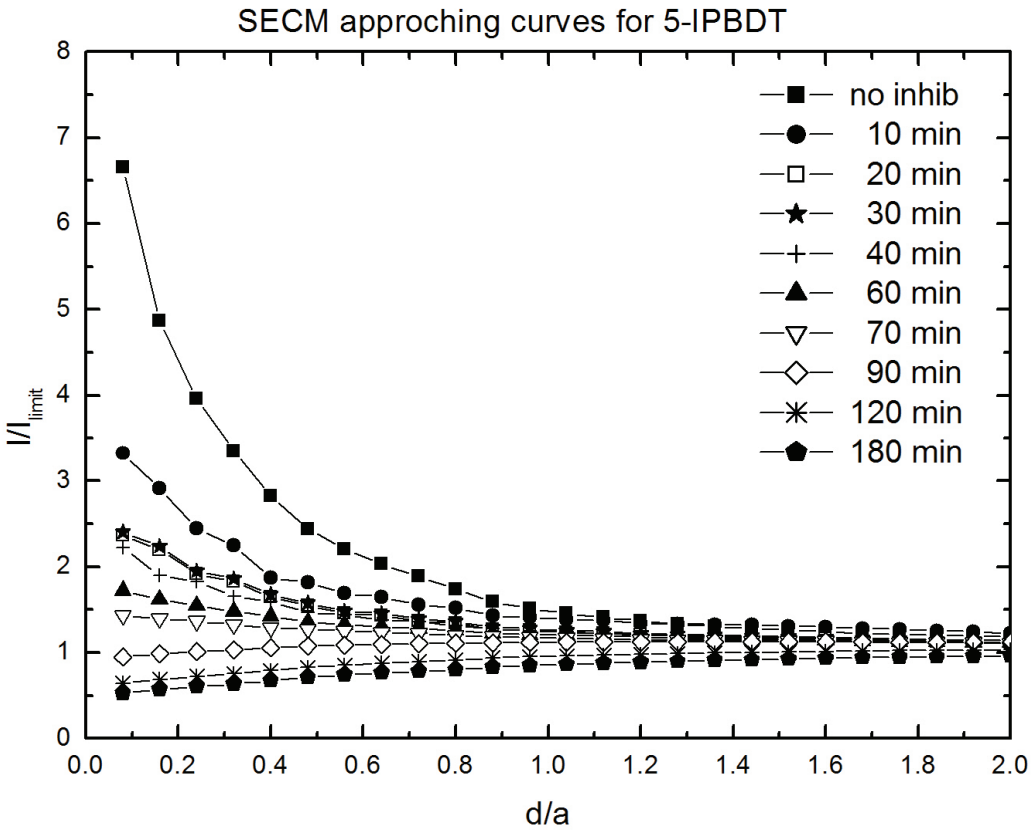

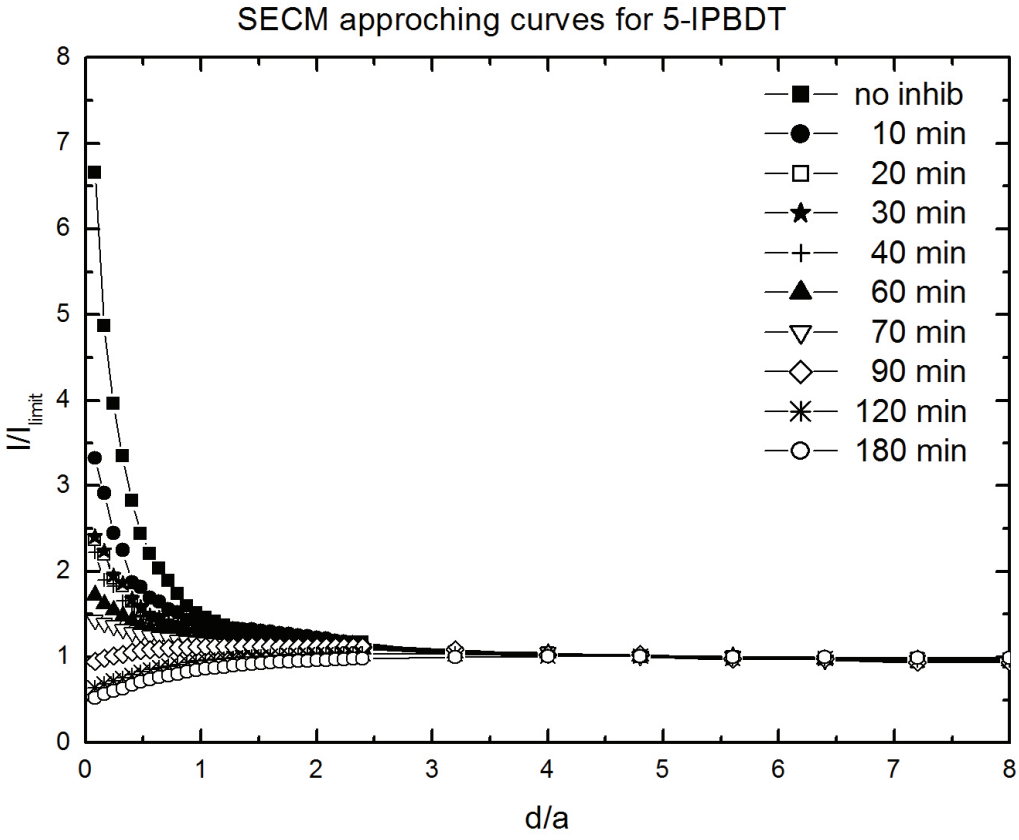

Figure 2 a, b. The approach curves measured *in-situ* at the copper substrate in IPBDT-containing electrolyte with a commercial 25 μm Au electrode. Electrolyte solution: 0.1 M Na_2SO_4 + 0.01 mM IPBDT + 0.67 mM FeMeOH. As a solution without inhibitor 0.67 mM FeMeOH solution was used. Tip potential: +0.5 V Ag/AgCl/KCl (saturated) reference electrode. Figure 2 b is the same as in 2 a, with smaller scale of the X axis.

The activity of the metal has been changed by the formation of the inhibitor layer. Both positive and negative feed-back (conducting and insulating surface) was obtained during the experiment. The conductive behavior of uncovered copper changed to an insulating surface due to the inhibitor layer formation.

The progresses of inhibitor layer formation in time was proved by the change of the shape of approach curves and by the decrease of the normalized current value measured at a distance of maximum approach (Figure 3).

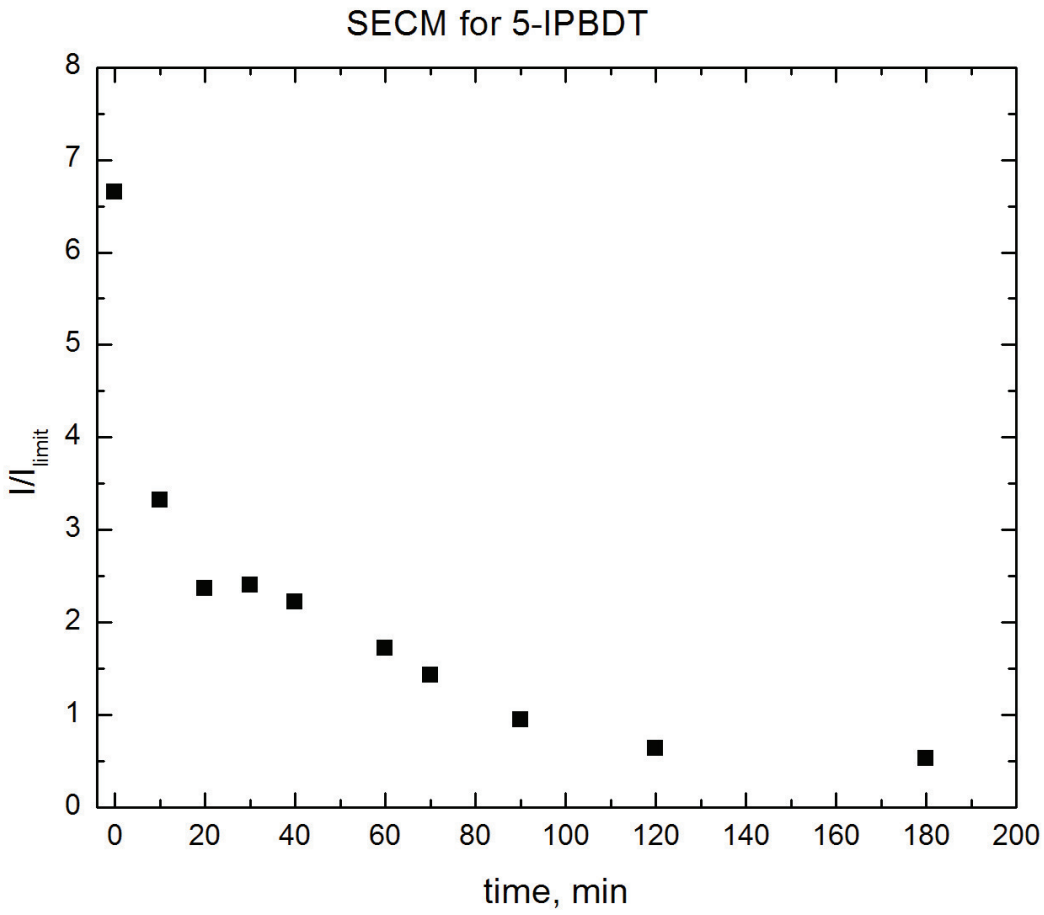

Figure 3. Change in time of the normalized current values measured at the closest distance (0.08 μm) of the tip from the surface

EQCM results:

Effect of corrosion inhibitors on Cu corrosion breakdown potential

The corrosion breakdown potential (E_b) is one of the most valuable parameters in providing the means for a quick and reliable comparison of the efficiency of various potential corrosion inhibitors. The breakdown potential is not a static parameter and is normally determined under dynamic conditions, usually using a linear potential scan voltammetry. This technique gives us an indication on the onset of anodic current, however, it is not possible to distinguish between the actual metal dissolution or metal oxide (or salt) scale build-up. Therefore, we applied the EQCM technique and monitored simultaneously the apparent mass variation and current change as a function of potential which was scanned in the anodic direction.

Inhibitors containing solutions were applied and results (i-E, Δm-E) were registered after the measuring system stabilized, i.e. there is no change in visco-elastic properties at the interface during measurement. The potential scan rate of cyclic voltammetric measurements was 1 mV/s. The potentials were swept as follows: E_1 = -500 mV, E_2 = 100 mV, E_3 = 0 mV and $E_4 = E_1$= -500 mV vs. SCE.

For Cu in the blank 0.1 M Na_2SO_4 solution:

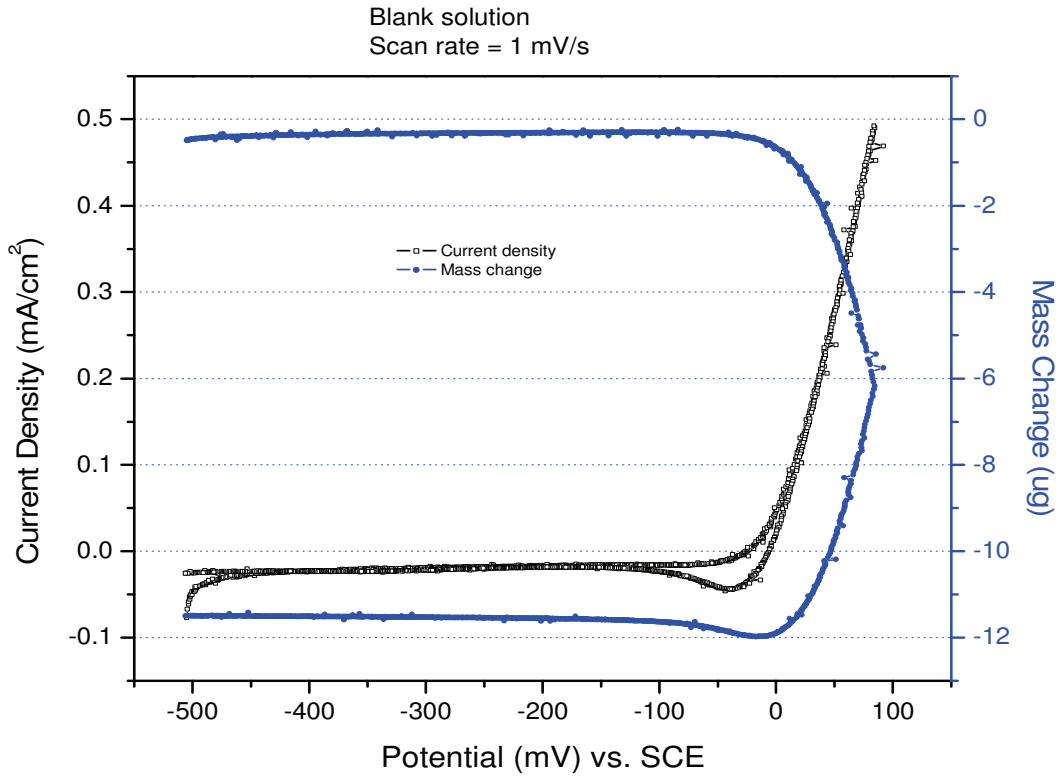

For Cu in 0.1 M Na_2SO_4 solution + 5-IPBDT:

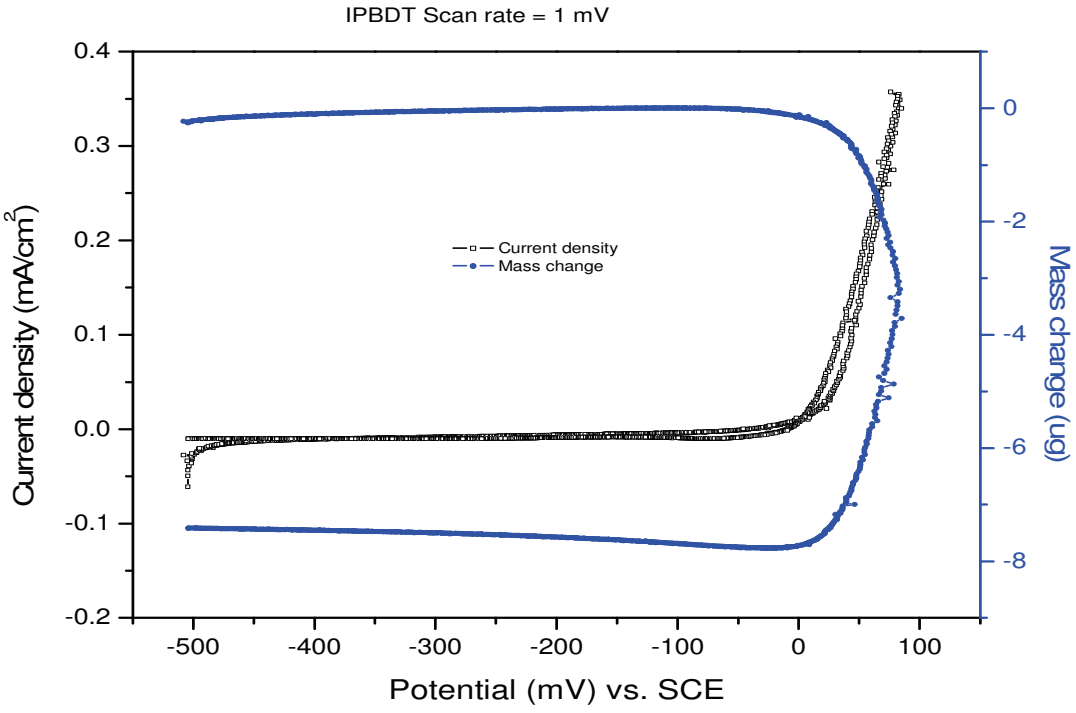

For Cu in 0.1 M Na_2SO_4 solution + 5-BDT:

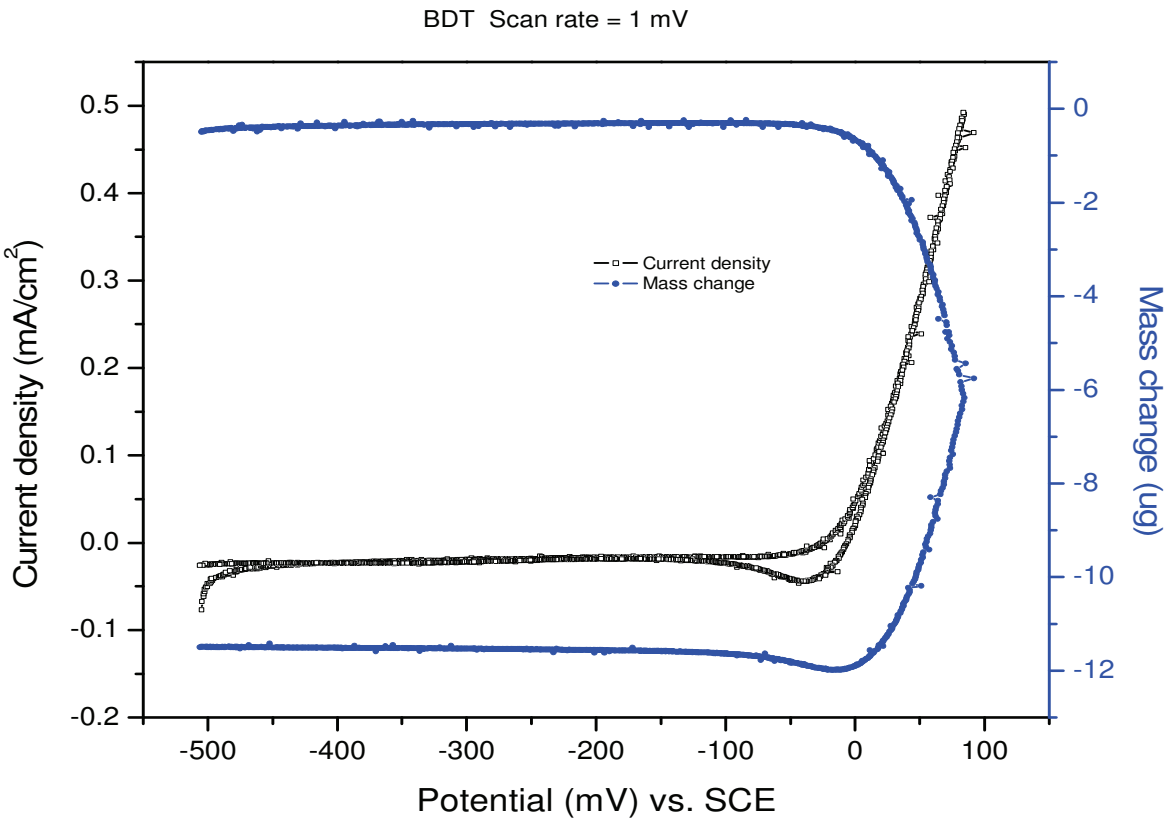

For Cu in 0.1 M Na_2SO_4 solution + 5-MBDT:

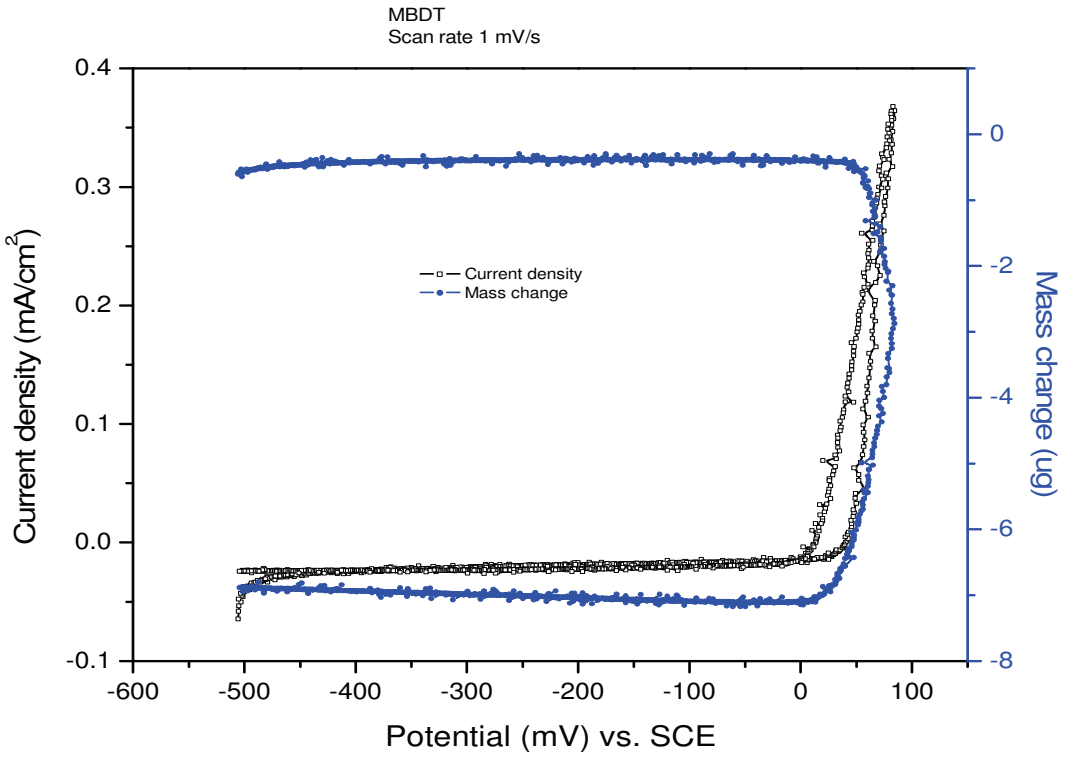

For Cu in 0.1 M Na_2SO_4 solution + 5-TDT:

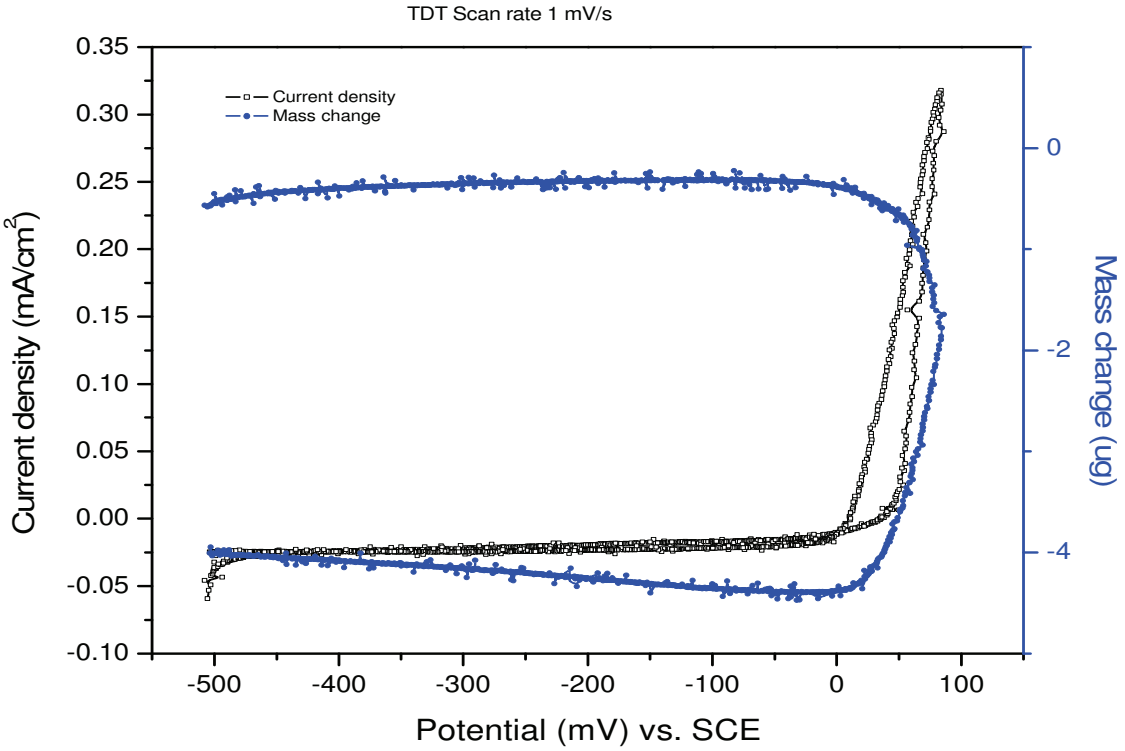

To summarize the EQCM results for a comparison reasons we present the following figures:

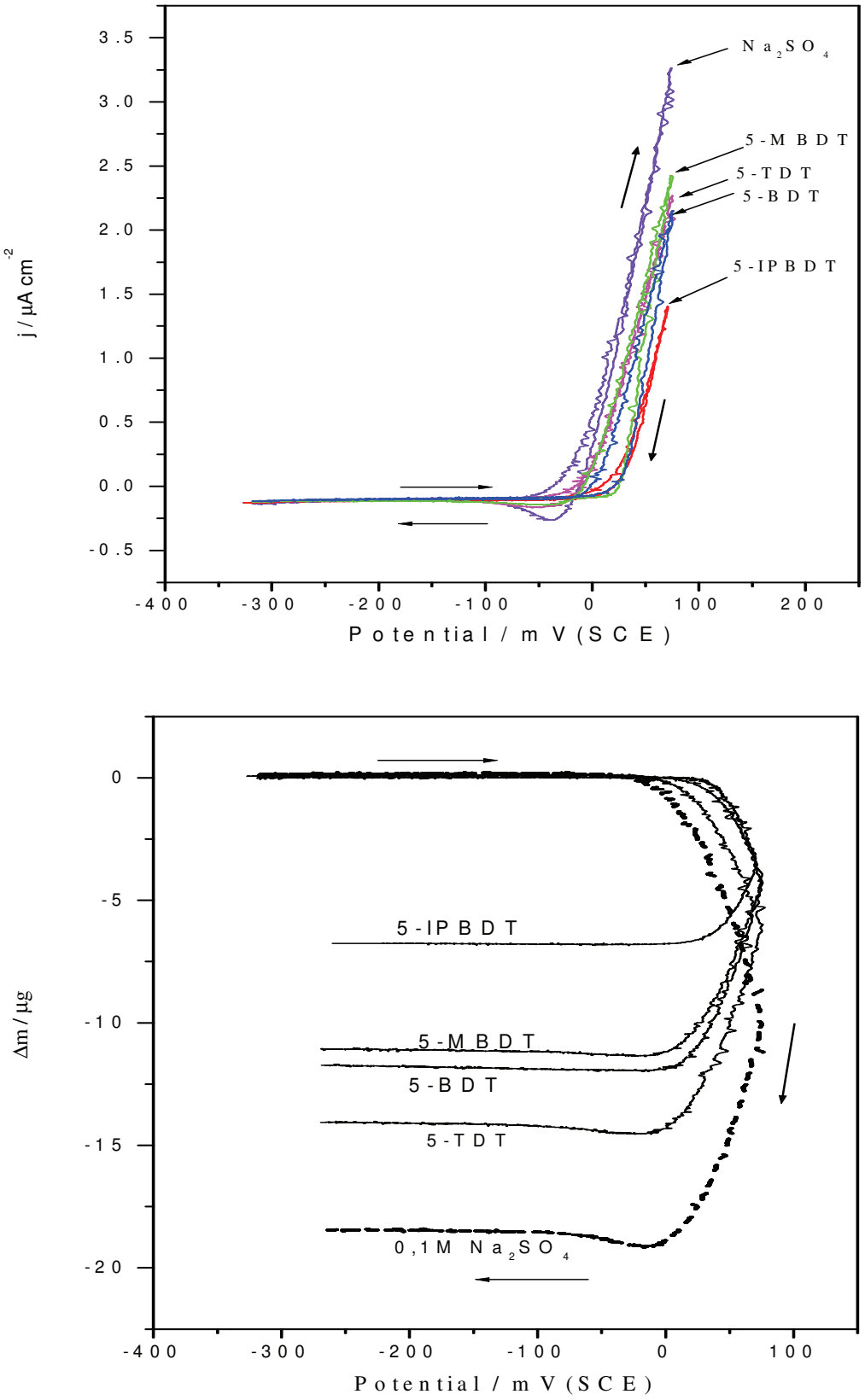

Figure 4. Linear potential scan voltammetric (4a) and piezogravimetric (4b) characteristics of a fresh thiazole films on a Cu-EQCM electrode in 0.1 M Na_2SO_4 + 0.01mmol/dm^3 of the thiazole derivatives solution, recorded at a scan rate =1 mV s^{-1}.

Figure 4 shows voltammetric (Fig. 4a) and piezogravimetric (Fig. 4b) characteristics of fresh Cu-EQCM electrode surfaces in 0.1 M Na_2SO_4 + 0.01 mmol.dm^{-3} of the thiazole derivatives solution, recorded at a scan rate = 1 mV s^{-1}. The electrode potential was scanned starting from E=–200 mV, to -300 mV, to 100 mV and back to –300 mV, vs. SCE. It is seen that the anodic current begins to flow after passing E= - 36 mV in the case of the blank solution. The addition of the thiazole derivatives shifted the break potential to more positive values (E_b= +8 for IPBDT, +20 for BDT, +25 for MBDT and –16 for TDT) as shown in Table 2. Among the tested thiazoles derivatives, 5-IPBDT produced the highest positive shift of the breaking potential.

Table 2. Characteristics of the Cu electrode immersed in 0.1 M Na_2SO_4 with the addition of different thiazole derivatives at a concentration of 0.01mmol.dm^{-3}.

Inhibitor	**E_b (mV)**	**ΔE (mV)**	**Δm (μg)**	**i_{max} (mA/cm^2)**
0.1 mol.dm^{-3} Na_2SO_4	-36	0	-18.5	3.27
0.01 mmol.dm^{-3} 5-IPBDT	+8	44	-6.75	1.40
0.01 mmol.dm^{-3} 5-BDT	+20	56	-11.7	2.15
0.01 mmol.dm^{-3} 5-MBDT	+25	61	-11.1	2.41
0.01 mmol.dm^{-3} 5-TDT	-16	20	-14.1	2.25

A simultaneous mass decrease is observed on m–E characteristic signifying that the copper dissolution is the predominant process above the breakdown potential. The copper dissolution continues up to the anodic reversal potential E=400 mV. On the return cathodic going scan, further dissolution is observed until E=30 mV and then is followed by a large mass increase concomitant with cathodic current flow. From the latter two observations, it can be concluded that the backward process is the electro-deposition of dissolved copper from the vicinity of the electrode surface. It can also be seen from Fig. 4 that the mass does not return to the initial level but to a higher level by ca. 0.15 μg. This mass imbalance may be due to several effects:

- the growth of copper (II) oxide and oxysalts which have a low electric conductance and are not completely reduced in the cathodic potential scan;
- increase in the surface roughness factor caused by the copper dissolution/redeposition processes and inclusion of water in the surface pores; and,
- formation of an inhibiting film (CuBTA) which in this case may also contain Cu(I) compounds such as CuCl and Cu_2O.

CONCLUSIONS

The inhibition effectiveness of thiazole derivatives was studied. For this purpose electrochemical (EIS and SECM) and electro-gravimetrical measurements were performed.

EQCM results showed linear potential scan voltammetric and piezogravimetric characteristics of a fresh thiazole films on a Cu electrode in 0.1 M Na_2SO_4 + 0.01mmol dm^{-3} of the thiazole derivatives solution, recorded at a scan rate =1 mV s^{-1}.

SECM results showed some promising results concerning the formation of the inhibitor protective layer in time.

The applied techniques showed that 5-IPBDT, among the tested thiazole derivatives, produced excellent protection against copper corrosion in acidic Na_2SO_4 solution. The effective protection of 5-IPBDT can be related to the presence of a longer chain and also the presence of the isopropyl group. Presence of other thiazole derivatives also hindered the copper corrosion.

REFERENCES

1. F. Mansfeld, ed., Corrosion Mechanisms, New York, NY: Marcel Dekker, (1987), p.119.
2. G. Trabanelli, Corrosion 47, 6 (1991): p. 410.
3. L. Kiss, Kinetics of Electrochemical Metal Dissolution (Amsterdam, NL: Elsevir, 1988).
4. A. Shaban, E. Kálmán and J. Telegdi, Electrochim. Acta, 43, 159-163 (1998)
5. A. Jardy, A. Legal Lasalle-Molin, M. Keddam, H. Takenouti, Electrochim. Acta 37 (1993): p. 2195.
6. *M. M. Antonijevic* and M. B. Petrovic, Int. J. Electrochem. Sci.,* 3 **(2008)** 1 - 28
University of Belgrade, Technical Faculty Bor 19210 Bor, P. Box 50, VJ 12, Serbia
7. J. Uehara, H. Nishihara, K. Aramaki, J. Electrochem. Soc. 137 (1990): p. 2677.
8. J. Uehara, K. Aramaki, J. Electrochem. Soc. 138 (1991): p.3245.
9. M. Itoh, H. Nishihara, K. Aramaki, J. Electrochem. Soc. 141 (1994): p. 2018.
10. M. Itoh, H. Nishihara, K. Aramaki, J. Electrochem. Soc. 142 (1995): p.1839.
11. Y. Yamamoto, H. Nishihara, K. Aramaki, J. Electrochem. Soc.140 (1993): p. 436.
12. O. Hollander, G. Dronne, J. Briquet, S. Dunn, M. Fealy, Proceedings of the 7th European Symposium on Corrosion Inhibitors, (Ferrara: Italy, 1990), p. 517.
13. A. Shaban, E. Kálmán, J. Telegdi, Gy. Dóra**,** J. Appl. Phys. A66 545-549 (1998)
14. N. Ohno, J. Uehara, K. Aramaki, J. Electrochem. Soc. 140 (1993): p.2512.
15. E. Szőcs, Gy. Vastag, A. Shaban, G. Konczos, E. Kálmán, J. Appl. Electrochem. 29., 1339-1345 (1999)
16. A. Shaban, E. Kálmán, J. Bácskai, Proceedings of the 8th European Symposium on Corrosion Inhibition, (Ferrara: Italy, 1995), p.951
17. D. Jope, J. Sell, H. W. Pickering, K. G. Weil, J. Electrochem. Soc. 142 (1995): p. 2170.
18. J. Telegdi, A. Shaban, E. Kálmán:, Electrochim. Acta, 45 No. 22-23 (2000) 3639.
19. G. Sauerbrey, Z. Phys. 155 (1959): pp. 206.
20. S. Bruckenstein, M. Shay, Electrochim. Acta 30 (1985): p.1295.
21. R. Kazinczi, E. Szőcs, E. Kálmán, P. Nagy, Appl. Phys. A66 (1998) 535-538
22. Gy. Vastag, E. Szőcs, A. Shaban, I. Bertóti, K. Popov-Pergal, E. Kálmán: Solid State Ionics, (2001) pp 87-91.